ASTRONOMY & ASTROPHYSICS
SUPPLEMENT SERIES

*Astron. Astrophys. Suppl. Ser.* **141**, 211–220 (2000)



# Structure and stellar content of dwarf galaxies⋆

## IV. *B* and *R* photometry of dwarf galaxies in the CVnI cloud

**T. Bremnes**[1], **B. Binggeli**[1], **and P. Prugniel**[2]

[1] Astronomical Institute, University of Basel, Venusstrasse 7, CH-4102 Binningen, Switzerland
[2] Observatoire de Lyon, F-64561 St. Genis-Laval Cedex, France

Received October 8; accepted October 25, 1999

**Abstract.** We have carried out CCD photometry in the Cousins $B$ and $R$ bands of 15 galaxies in the Canes Venatici I cloud. Total magnitudes, effective radii, effective surface brightnesses, as well as galaxy radii at various isophotal levels in both colors were determined. Best-fitting exponential parameters and color gradients are also given for these galaxies. The photometric parameters presented here will be analyzed in a forthcoming paper, together with previously published data for nearby dwarf galaxies.

**Key words:** galaxies: general — galaxies: fundamental parameters — galaxies: photometry — galaxies: irregular — galaxies: structure — galaxies: luminosity function

### 1. Introduction

Continuing a series of papers on dwarf galaxies within 10 Mpc (Bremnes et al. 1998; Lesaffre et al. 1999; Bremnes et al. 1999), hereafter Papers I, II and III, we here present photometric data on dwarf galaxies in the Canes Venatici I cloud (CVnI). The cloud is composed of some 40 galaxies distributed in the region of the sky delimited by $11\overset{\mathrm{h}}{.}5 < \alpha < 14\overset{\mathrm{h}}{.}0$, $+20° < \delta < +60°$ (Makarova et al. 1998) and has a mean heliocentric radial velocity of $<v_{\mathrm{hel}}> \approx 300$ km s$^{-1}$. A map showing the distribution of these objects on the sky is shown by Makarova et al. (1998) in their Fig. 1. The structure of the cloud is somewhat different from the groups studied in Papers I, II and III in that there is no dominant galaxy, like in the M 81 or M 101 groups. It is constituted of several loose aggregations of galaxies, mostly of late types. This study therefore complements Papers I, II and III towards globally lower density environments. Accurate distances are becoming available as photometric distance determinations[1] (Makarova et al. 1997; Georgiev et al. 1997; Tikhonov & Karachentsev 1998; Makarova et al. 1998; Karachentsev & Drozdovsky 1998). The combination of distance information and photometry will enable a thorough study of the photometric parameters of these systems.

In the following section we describe the sample and the imaging, in Sect. 3 we describe the reduction procedure. The results are presented in Sect. 4. Model-free parameters, i.e. total magnitudes, effective radii and effective surface brightnesses were determined in the Cousins $B$ and $R$ bands. Best fitting exponential model parameters, i.e. extrapolated central surface brightness and exponential scale length were also determined. Finally, color gradients were measured for all but two galaxies lacking images in both colors. The tables and profile data in electronic format are available from us on request.

### 2. Sample and imaging

The photometry of the objects listed in Table 1 is based on images taken during a 14-night run in March 1998 on the 1.2 m telescope of the Observatoire de Haute-Provence (OHP). Unfortunately, half of the nights were lost due to bad weather, so the total amount of galaxies successfully imaged was 15. The frames are 40 minute $B$ and 20 minute $R$ exposures. We used the No. 2 Tektronix $1024 \times 1024$ CCD camera. The pixel scale is $0\overset{''}{.}69^{-1}$, giving a frame size of $11\overset{'}{.}8 \times 11\overset{'}{.}8$. The gain was set to $3.5\,\mathrm{e}^-$ per ADU, and the CCD was read out in the fast mode, with a readout noise of $8.5\,\mathrm{e}^-$. Seeing was generally fair to poor, between $2\overset{''}{.}5$ and $4\overset{''}{.}5$, but for our purposes the images were

*Send offprint requests to*: T. Bremnes,
e-mail: bremnes@astro.unibas.ch

⋆ Based on observations made at Observatoire de Haute Provence (CNRS), France.

[1] Radial velocities are not reliable distance indicators for nearby galaxies because of possibly large peculiar velocities.

**Table 1.** CVnI galaxies observed. See text for explanations

| No. | Ident. 1 | Ident. 2 | R.A. | Dec. | Type | $B_T$ | $V_{hel}$ | Dist. |
|---|---|---|---|---|---|---|---|---|
| 1. | UGC 06541 | UGC 06541 | 11h33′29.″12 | +49°14′17.″4 | SmIII/BCD[b] | 14.32 | 249 | 3.5[3] |
| 2. | NGC 3738 | UGC 06565 | 11h35′48.″47 | +54°31′27.″9 | Irr | 11.92 | 229 | 3.5[3] |
| 3. | NGC 3741 | UGC 06572 | 11h36′06.″18 | +45°17′01.″1 | ImIII/BCD[b] | 14.38 | 229 | 3.5[3] |
| 4. | DDO 99 | UGC 06817 | 11h50′52.″99 | +38°52′49.″0 | Im | 13.45 | 243 | 3.9[3] |
| 5. | NGC 4068 | UGC 07047 | 12h04′02.″39 | +52°35′24.″1 | SmIII/BCD[b] | 12.93 | 210 | 5.25[4] |
| 6. | NGC 4150 | UGC 07165 | 12h10′33.″36 | +30°24′11.″8 | SA(r) | 12.41 | 226 | |
| 7. | NGC 4163 | UGC 07199 | 12h12′09.″15 | +36°10′09.″1 | BCD[b] | 13.66 | 165 | 3.6[2] |
| 8. | DDO 113 | UGCA 276 | 12h14′57.″92 | +36°13′07.″8 | dE3[b] | 15.70 | 284 | 4.1[4] |
| 9. | UGC 07298 | UGC 07298 | 12h16′28 | +52°15′.3 | ImIV?[b] | 15.96 | 172 | 8.6[2] |
| 10. | NGC 4248 | UGC 07335 | 12h17′50.″36 | +47°24′30.″6 | d:S0[b] | 13.13 | 484 | |
| 11. | UGC 07356 | UGC 07356 | 12h19′09.″6 | +47°05′29″ | dE4,N[b] | 15.58 | 272 | unr[1] |
| 12. | IC 779 | UGC 07369 | 12h19′38.″76 | +29°53′00.″2 | E | 14.84 | 333 | |
| 13. | DDO 126 | UGC 07559 | 12h27′05.″15 | +37°08′33.″3 | Sdm[b] | 14.2 | 218 | 5.1[1] |
| 14. | DDO 127 | UGC 07599 | 12h28′28.″56 | +37°14′01.″1 | Sm | 14.80 | 278 | 6.9[1] |
| 15. | UGC 07639 | UGC 07639 | 12h29′53.″04 | +47°31′47.″9 | dS0/BCD[b] | 13.94 | 382 | 8.0[1] |

still useful. The data collected in Table 1 consists of the identification of the imaged galaxies in Cols. 2 and 3, their 2000.0 epoch coordinates in Cols. 4 and 5, types in Col. 6, with classification from Binggeli et al. (1990) marked with [b], total $B$ magnitude from the present photometry, except for galaxy #13, in Col. 7, heliocentric radial velocity in Col. 8 and photometric distances in the last column. All data except for those of the last column, the magnitudes and type data marked with [b] are taken from the NED. The photometric distances are from Makarova et al. (1997, 1998)[1,4], Tikhonov & Karachentsev (1998)[2] and Georgiev et al. (1997)[3]. A gallery of our images is shown in Fig. 2.

## 3. Reductions

The photometry was done with the `MIDAS` package developed by `ESO`. The images were combined, bias-subtracted and flatfielded using standard procedures. The images were flat-fielded using combined morning and evening twilight flat-fields as well as dome flats. The following reduction steps were done within the `SURFPHOT` context in `MIDAS`. The background was determined by fitting a tilted plane with `FIT/BACKGROUND` and was checked for correctness by measuring the sky level in different locations in the frames in regions unaffected by the objects. We chose to restrict the sky fitting to a tilted plane to avoid introducing features which are difficult to assess, as would be the case if we had used a polynomial fit. This also stresses the need for precise flat-fielding. The photometric calibration was done using standard methods. The calibration fields were chosen to be close on the sky to the observed galaxies. These were taken from Smith et al. (1985). The calibration stars were imaged before and after imaging every second galaxy, so one could have a handle on eventual transparency variations on a time scale of two hours. For each galaxy the center and the ellipse-fit parameters, i.e. ellipticity and position angle (counted counter-clockwise from the horizontal axis), were determined at the level of $\sim 25^{\rm th}$ mag/□″ by the ellipse fitting routine `FIT/ELL3` and are given in Table 2. These parameters were used to obtain the total light profile, i.e. growth curve, by integrating the galaxy light in elliptical aperture of fixed ellipticity and position angle but with increasing equivalent ($r = \sqrt{ab}$) radius. Bright sources were removed by hand from the frames before integrating the light.

**Table 2.** Ellipse fit parameters at the level of 25 mag/□″

| No. | Galaxy | PA [°] | $a$[″] | $b$[″] | $b/a$ |
|---|---|---|---|---|---|
| 1. | UGC 06541 | 039 | 39.9 | 21.2 | 0.5 |
| 2. | UGC 06565 | 069 | 91.0 | 71.6 | 0.8 |
| 3. | UGC 06572 | 105 | 35.9 | 27.8 | 0.8 |
| 4. | UGC 06817 | 150 | 84.1 | 39.2 | 0.5 |
| 5. | UGC 07047 | 123 | 81.3 | 46.4 | 0.6 |
| 6. | UGC 07165 | 057 | 61.6 | 43.2 | 0.7 |
| 7. | UGC 07199 | 094 | 53.0 | 35.2 | 0.7 |
| 8. | UGCA 276 | 126 | 53.8 | 34.1 | 0.6 |
| 9. | UGC 07298 | 047 | 23.0 | 15.3 | 0.7 |
| 10. | UGC 07335 | 020 | 87.6 | 37.6 | 0.4 |
| 11. | UGC 07356 | 062 | 25.9 | 17.6 | 0.7 |
| 12. | UGC 07369 | 151 | 29.9 | 24.2 | 0.8 |
| 13. | UGC 07559 | 056 | 64.5 | 38.1 | 0.6 |
| 14. | UGC 07599 | 038 | 43.5 | 22.4 | 0.5 |
| 15. | UGC 07639 | 056 | 56.3 | 30.2 | 0.5 |

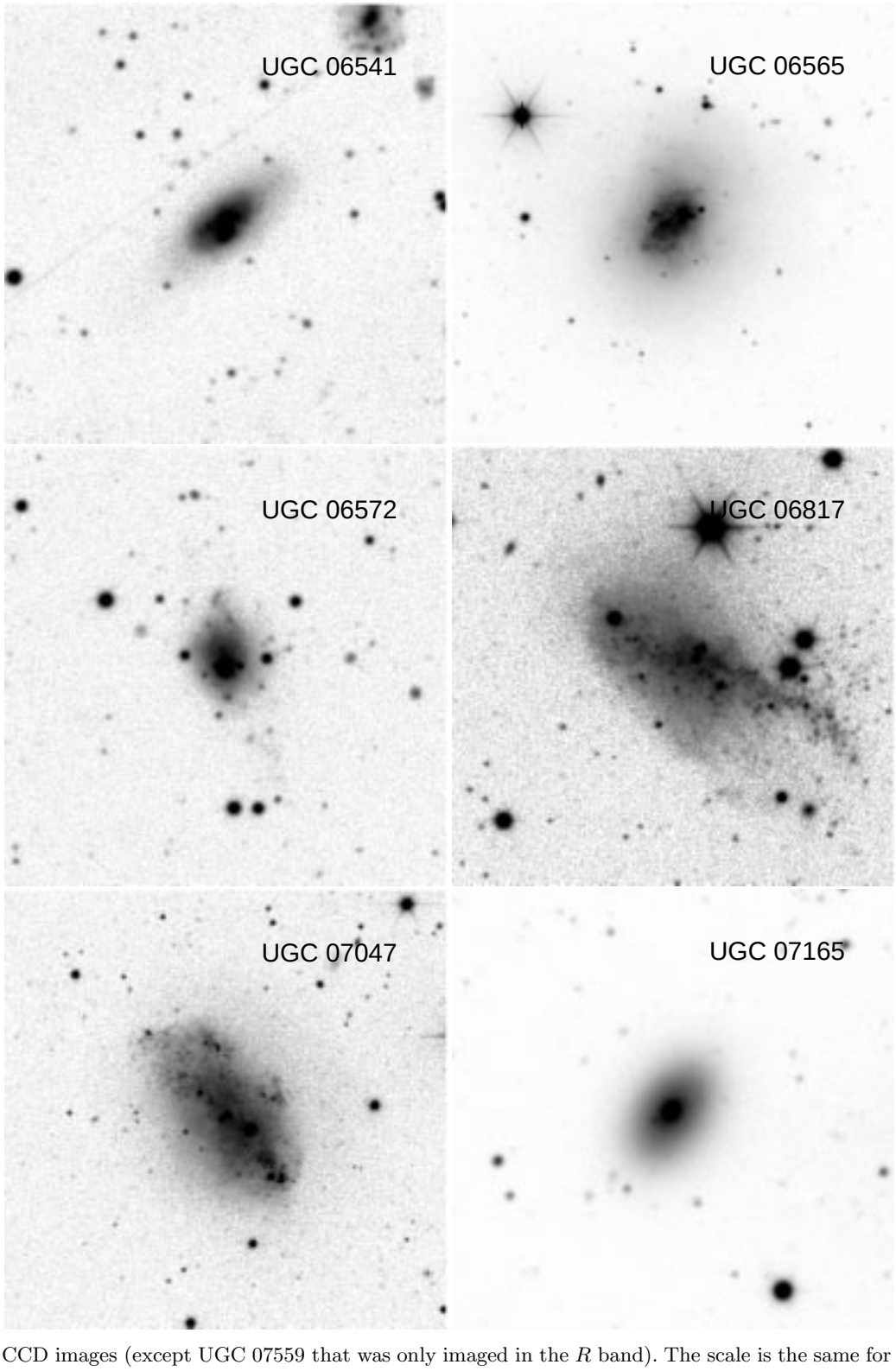


**Fig. 2.** *B*-band CCD images (except UGC 07559 that was only imaged in the *R* band). The scale is the same for all pictures and is given by the size of one image side = 5′.9. North is up and east to the left

## 4. Results

### *4.1. Model-free photometric parameters and radial profiles*

The global photometric parameters of our objects are listed in Table 3, and the columns represent: the galaxies number ordered by increasing right ascension (1), name of the galaxy (2), total apparent magnitude in the *B* band (3), total apparent magnitude in the *R* band (4), effective radius in *B* in arcsec(5), effective radius in *R* in arcsec (6),

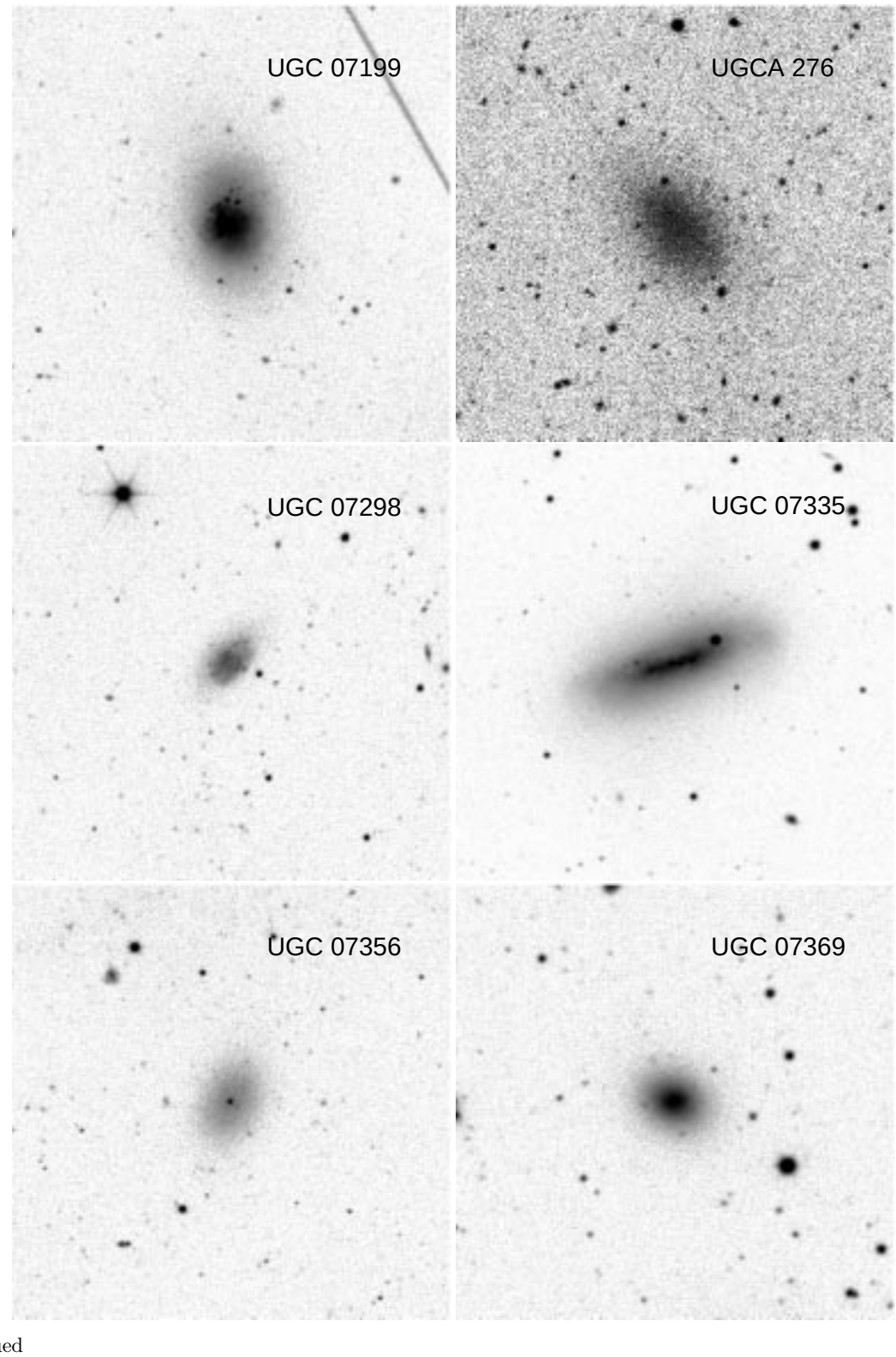


**Fig. 2.** continued

effective surface brightness in $B$ [mag/$\Box''$] (7), effective surface brightness in $R$ [mag/$\Box''$] (8) , total $B-R$ color index (9) and galactic absorption in $B$ from the NED (10).

The total apparent magnitude of a galaxy was read off the growth curve at a sufficiently large radius, i.e. where the growth curve becomes asymptotically flat. The model-free effective radius was then read at half of the total

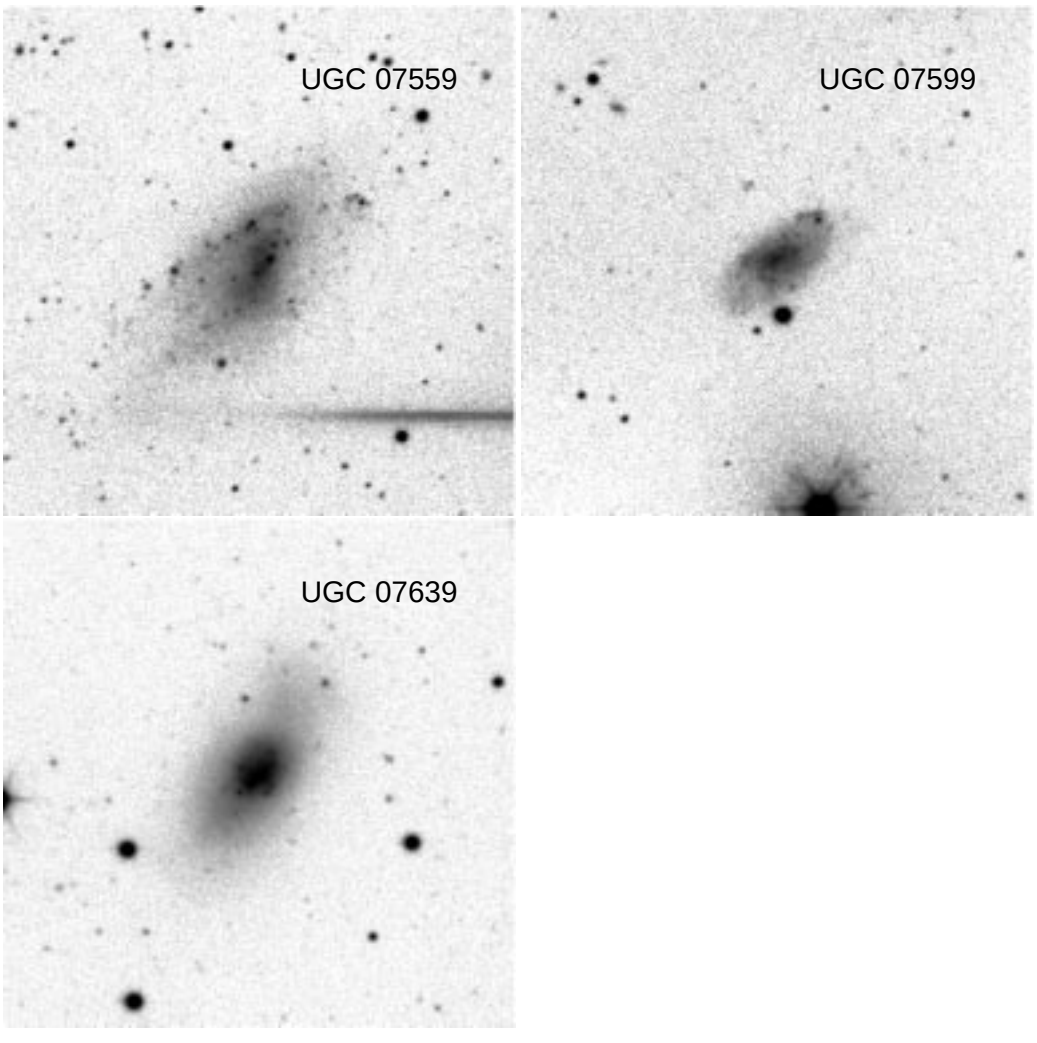


**Fig. 2.** continued

growth curve intensity. The effective surface brightness is then given by

$$<\mu>_{\rm eff}[{\rm mag}/\Box''] = M + 5\log(R_{\rm eff}[''])+2. \quad (1)$$

All radii refer to equivalent radii, $r=\sqrt{ab}$, where $a$ and $b$ are the major and minor axis of the galaxy, respectively. Surface brightness profiles were obtained by differentiating the growth curves with respect to equivalent radius. The resulting $B$ and $R$ surface brightness profiles are shown in Fig. 3. The profiles are traced down to the level where the uncertainties owing to the fluctuations in the sky level on the profile become dominant. As discussed in Sect. 4.3, this represents approx. 28.5 mag/$\Box''$ in $B$ and 27.5 mag/$\Box''$ in $R$. Galactic absorption values were taken from the NED database. A correction for internal extinction was not applied, as it is not well known in the case if dwarf galaxies. The profiles drawn in the figures have been slightly smoothed with a running window of width $\approx 5''$ and are plotted on a linear radius scale.

Color profiles obtained by subtracting the $R$ from the $B$ surface brightness profiles, together with the difference between the slopes of exponential fits (dotted line, see Sect. 4.2) are plotted in Fig. 4.

### *4.2. The exponential model: Fits and parameters*

It is well accepted that the radial intensity profiles of dwarf galaxies can be reasonably well fitted by a simple exponential (De Vaucouleurs 1959; Binggeli & Cameron 1993). This applies not only for dwarf ellipticals, but also for irregulars, if one looks aside from the brighter star-forming regions and considers the underlying older populations. These profiles can be written as

$$I(r) = I_0\ \exp\left(-\frac{r}{r_0}\right) \equiv I_0\,{\rm e}^{-\alpha r}, \quad (2)$$

that in surface brightness representation becomes a straight line

$$\mu(r) = \mu_0 + 1.086\,\alpha r. \quad (3)$$

The central extrapolated surface brightness $\mu_0$ and the exponential scale length $1/\alpha$ are the two free parameters

**Table 3.** Global photometric properties. See text for explanations

| No. | Galaxy | $B_{\rm T}$ | $R_{\rm T}$ | $r_{\rm eff}^{B}$ | $r_{\rm eff}^{R}$ | $<\mu>_{\rm eff}^{B}$ | $<\mu>_{\rm eff}^{R}$ | $B-R$ | $A_B$ |
|---|---|---|---|---|---|---|---|---|---|
| 1. | UGC 06541 | 14.32 | 13.46 | 14.99 | 17.98 | 22.20 | 21.74 | 0.86 | 0.00 |
| 2. | UGC 06565 | 11.92 | 10.94 | 28.60 | 37.12 | 21.20 | 20.79 | 0.98 | 0.00 |
| 3. | UGC 06572 | 14.38 | 13.57 | 16.30 | 19.92 | 22.44 | 22.07 | 0.81 | 0.00 |
| 4. | UGC 06817 | 13.45 | 12.61 | 53.41 | 61.37 | 24.09 | 23.55 | 0.85 | 0.00 |
| 5. | UGC 07047 | 12.93 | 11.93 | 42.00 | 46.14 | 23.05 | 22.25 | 1.00 | 0.00 |
| 6. | UGC 07165 | 12.41 | 11.11 | 16.09 | 15.52 | 20.44 | 19.06 | 1.30 | 0.04 |
| 7. | UGC 07199 | 13.66 | 12.65 | 22.92 | 27.39 | 22.46 | 21.83 | 1.02 | 0.00 |
| 8. | UGCA 276 | 15.70 | 14.58 | 38.24 | 37.69 | 25.62 | 24.46 | 1.13 | 0.00 |
| 9. | UGC 07298 | 15.96 | 15.25 | 13.46 | 15.70 | 23.61 | 23.23 | 0.72 | 0.04 |
| 10. | UGC 07335 | 13.13 | 11.87 | 29.66 | 31.01 | 22.49 | 21.33 | 1.26 | 0.00 |
| 11. | UGC 07356 | 15.58 | 14.21 | 23.78 | 26.61 | 24.46 | 23.33 | 1.37 | 0.00 |
| 12. | UGC 07369 | 14.84 | 13.46 | 16.07 | 17.30 | 22.87 | 21.65 | 1.38 | 0.07 |
| 13. | UGC 07559 | | 13.55 | | 35.86 | | 23.32 | | 0.00 |
| 14. | UGC 07599 | 14.80 | | 22.15 | | 23.52 | | | 0.00 |
| 15. | UGC 07639 | 13.94 | 12.93 | 26.11 | 31.64 | 23.02 | 22.43 | 1.01 | 0.00 |

of the exponential fit. In this work the fits to the profiles were done on the outer parts of the profiles by a least squares fitting procedure. The best-fitting parameters are listed in Table 4. The best-fitting exponential profiles are plotted as dash-dotted lines along with the observed profiles in Fig. 3. The deviation from a pure exponential law is expressed by the difference $\Delta M$ between the total magnitude of an exponential intensity law given by

$$M_{\rm exp} = \mu_0^{\rm exp} + 5\log\alpha - 2.0, \quad (4)$$

and the actual measured total magnitude. The results are shown in Table 4. The difference shows the goodness of fit of the exponential intensity profile. The columns of Table 4 are as follows: (1) as Col. 1 of Table 3, (2) as Col. 2 of Table 3, extrapolated central surface brightness according to Eq. (3) in $B\,[\mathrm{mag}/\Box'']$ (3), same in $R$ (4), exponential scale length in $B\,['']$ (5), same in $R$ (6), difference between the total magnitude as derived from the exponential model and the true total magnitude in $B$ (7), same in $R$ (8), radial color gradient determined from the difference in the slopes of the model fits as described in Sect. 4 [mag/''] (9).

### *4.3. Photometric uncertainties*

The photometric calibration represents the greatest source of error on the global parameters. The nights were not photometric, so calibrations were done with fields close on the sky to the actual objects, see Sect. 3. Some nights were rejected altogether because of the changing transparency on short time scales. The combined (zero point and slope of the extinction curve) statistical uncertainty on the photometric calibration is estimated to be about 0.1 mag. The uncertainties on the surface brightness profiles (SBP) are a combination of Poisson noise and, at low levels, the large-scale sky fluctuations, owing to flat fielding and sky subtraction imprecision. The uncertainties shown in Fig. 3 have been calculated assuming the galaxies have pure exponential SBPs. To the Poisson noise caused by the photons we added a constant contribution corresponding to 0.5% of the actual measured sky background, that combines the flat field and sky subtraction terms mentioned above. This level of accuracy for the flat fielding and sky subtraction was conservatively estimated by inspecting many frames. Most frames show better flat fielding accuracy. The uncertainties on the profiles were then calculated for azimuthally averaged annuli of one arc second width[2]. For the actual calculations, we considered circles instead of ellipses and compared equivalent radii when determining the error at a given point on a SBP. The galaxy surface brightness and the fluctuations in the sky background reach similar levels at $\sim 28.5$ in $B$ and $\sim 27.5\,\mathrm{mag}/\Box''$ in $R$.

The errors on the color profiles, shown in Fig. 4, were estimated using the error term as described above for each color and applying usual error formulae for logarithms and combining the errors thus obtained for each color by quadrature.

Comparing the $B$ magnitudes from this paper with RC3 data from the NED, one sees that our photometry agrees well with the RC3 for ten galaxies, see Fig. 5. Three galaxies, namely UGC 07199, UGC 07356 and UGC 07559 have brighter magnitudes and one, UGC 7298, has a fainter magnitude in this paper as compared to the values in the RC3. For a subsample of our galaxies, there are total magnitudes calculated by Makarova et al. (1997, 1998). Their data is shown in Fig. 5 as lozenges. The agreement between both photometries is better than for the RC3 data, especially for UGC 7356.

[2] The profiles in Fig. 3 have been smoothed for plotting, so the error-bars apply to the original un-smoothed SBPs. Also, the calibration uncertainties are not shown in the plots.

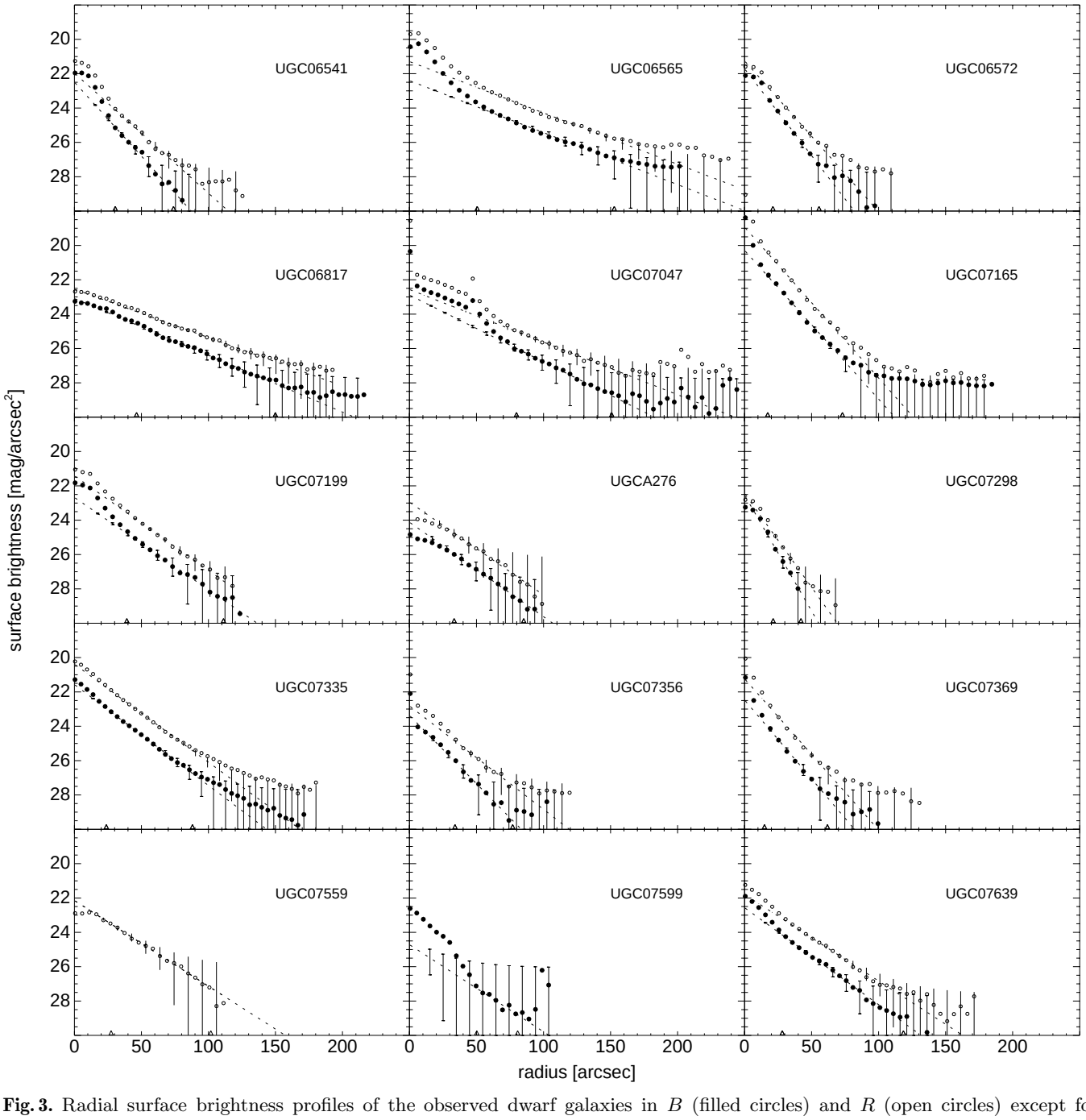


**Fig. 3.** Radial surface brightness profiles of the observed dwarf galaxies in $B$ (filled circles) and $R$ (open circles) except for UGC 7559 (only $R$) and UGC 7599 (only $B$). The central data point for UGC 7165 in $R$ is at 17.05 mag. The dotted lines represent the exponential fits, as described in Sect. 4.2, and the fitting region is marked by triangles on the $x$-axis. The error-bars are drawn with hats for the $B$ band data points and without for the $R$ band data points. These are calculated for (as described in Sect. 4.3), and are centered on the best-fitting exponentials. The radii are all equivalent radii ($r = \sqrt{ab}$)

## 5. Notes

The galaxies presented here have a median absolute magnitude of −14.43 mag. There are no very faint dwarf galaxies in this sample (see Fig. 5, compare with Paper I). The lowest magnitude object, UGCA 276, is at −12.37 mag, and is classified as a dwarf elliptical.

*On individual galaxies*:

**UGC 6541**: small galaxy, with a light excess close to the center as compared to an exponential profile. As can be seen on the image, this can be a star-forming region or a superimposed star. The color profile shows no deviation in the region concerned by the bright object, so its nature

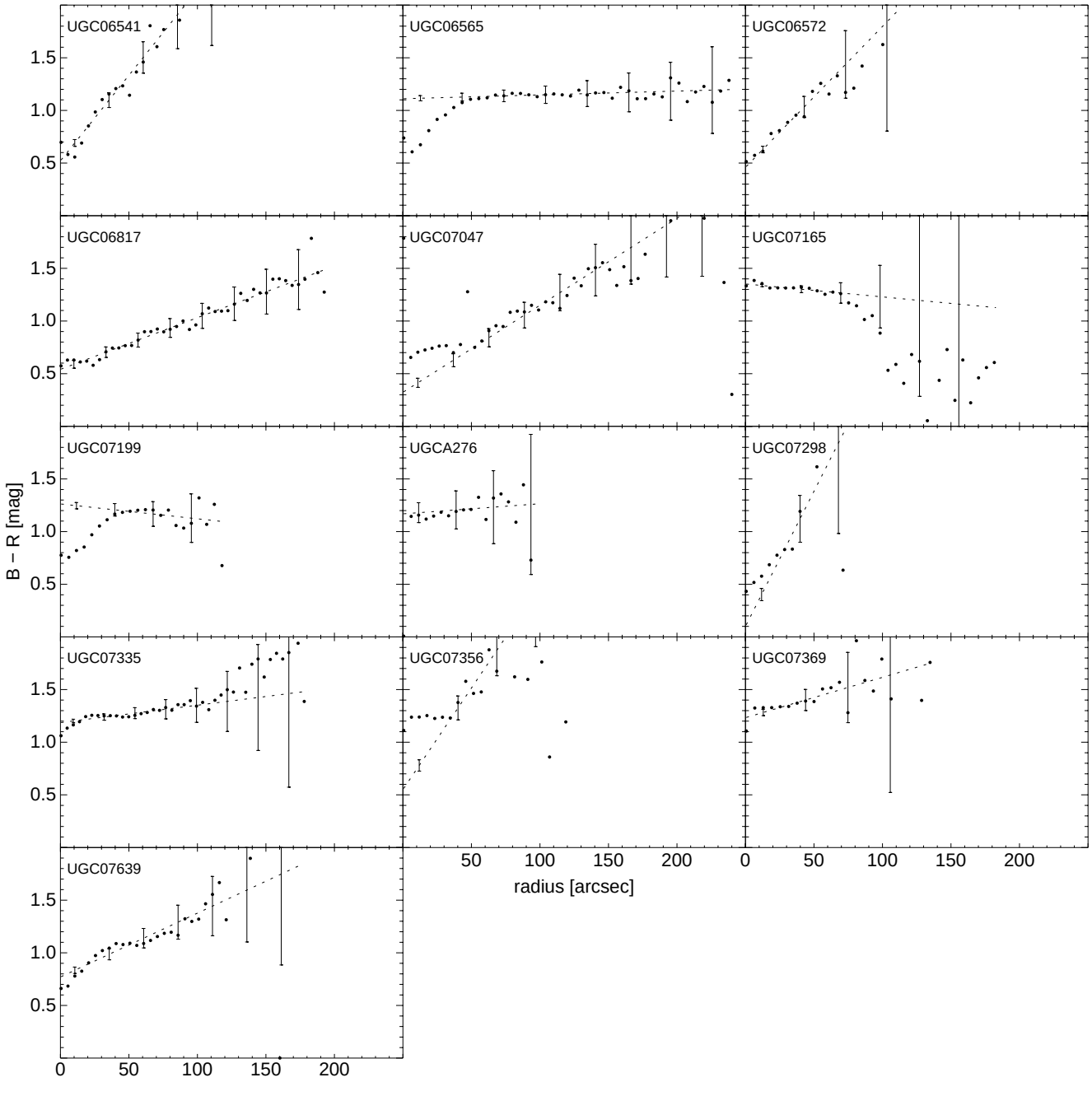


**Fig. 4.** Radial $B-R$ color profiles. The dotted lines represent the exponential fits, as described in Sect. 4.2. The error-bars have been computed as described in Sect. 4.3

is difficult to assess. The color gradient of this galaxy is steep, and in the sense of the center being bluer.

**UGC 6565**: possesses a bright central light excess above a pure exponential. This central part also has a knotty structure, and is also much bluer than the rest of the galaxy. This probably suggests ongoing star formation. The outer part of the galaxy seems smooth. The isophotes look boxy, although we haven't quantified this feature in this work.

**UGC 6572**: irregular structure, with a slightly offset bright region. The color profile is steep, but the brighter spot doesn't seem to be of a different color than its immediate surroundings.

**UGC 6817**: has a low central surface brightness and a large scale length. The SBP is close to a pure exponential, and the color gradient is smooth, showing a reddening with increasing radius. The aspect of the galaxy is peculiar, with a knotty irregular surface, and a tail extending to the

**Table 4.** Model parameters. See text for explanations

| No. | Galaxy | $(\mu_0^{\rm exp})_B$ | $(\mu_0^{\rm exp})_R$ | $1/\alpha_B$ | $1/\alpha_R$ | $\Delta M_B$ | $\Delta M_R$ | $\frac{{\rm d}(B-R)}{{\rm d}r}$ |
|---|---|---|---|---|---|---|---|---|
| 1. | UGC 06541 | 22.49 | 21.97 | 12.60 | 15.53 | 0.67 | 0.55 | 0.016 |
| 2. | UGC 06565 | 22.40 | 21.29 | 35.88 | 36.31 | 0.71 | 0.55 | 0.000 |
| 3. | UGC 06572 | 21.71 | 21.25 | 10.73 | 12.37 | 0.18 | 0.22 | 0.013 |
| 4. | UGC 06817 | 23.09 | 22.55 | 32.83 | 38.56 | 0.05 | 0.01 | 0.005 |
| 5. | UGC 07047 | 22.89 | 22.57 | 27.93 | 35.46 | 0.73 | 0.89 | 0.008 |
| 6. | UGC 07165 | 20.29 | 18.94 | 12.54 | 12.36 | 0.39 | 0.37 | −0.001 |
| 7. | UGC 07199 | 22.68 | 21.41 | 20.23 | 19.71 | 0.48 | 0.29 | −0.001 |
| 8. | UGCA 276 | 24.12 | 22.95 | 19.75 | 20.10 | −0.06 | −0.14 | 0.001 |
| 9. | UGC 07298 | 22.54 | 22.44 | 8.05 | 9.93 | 0.05 | 0.21 | 0.026 |
| 10. | UGC 07335 | 21.57 | 20.38 | 18.48 | 19.01 | 0.10 | 0.12 | 0.002 |
| 11. | UGC 07356 | 23.37 | 22.82 | 13.65 | 18.03 | 0.11 | 0.33 | 0.019 |
| 12. | UGC 07369 | 22.47 | 21.24 | 11.82 | 12.34 | 0.27 | 0.32 | 0.004 |
| 13. | UGC 07559 | | 22.14 | | 21.75 | | −0.09 | |
| 14. | UGC 07599 | 24.72 | | 21.41 | | 1.27 | | |
| 15. | UGC 07639 | 22.57 | 21.79 | 19.24 | 21.56 | 0.21 | 0.20 | 0.006 |

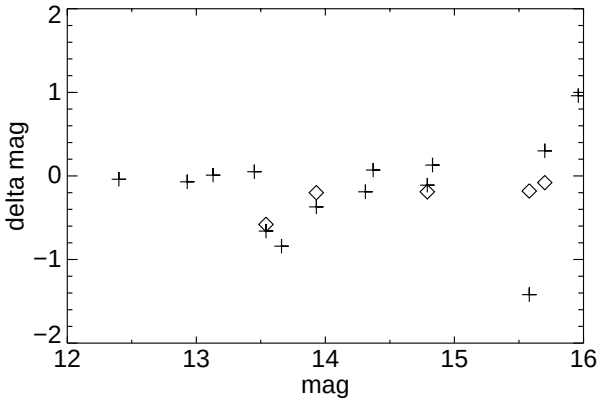


**Fig. 5.** Comparison between the photometry of the present paper and data from the RC3 catalog (crosses) and from Makarova et al. (lozenges). The $B$ magnitudes are from the present paper, and delta mag is the difference between our photometry and RC3 or Makarova et al. (1997, 1998)

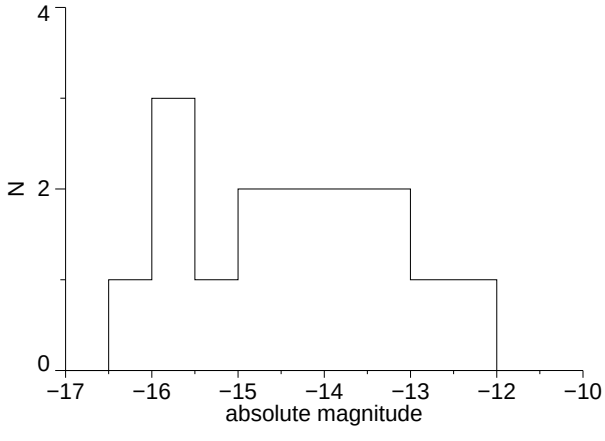


**Fig. 6.** Distribution of galaxy magnitudes. Distances are from Table 1. Where photometric distances were unavailable, the radial velocities were used with $H_0 = 60\,{\rm km\,s^{-1}\,Mpc^{-1}}$

south-west. It could have been disrupted by supernova events. The isophotes also seem twisted, although not examined in detail in this work.

**UGC 7047**: irregular with a knotty structure, and a light excess over an exponential profile towards the center. This part of the galaxy also shows a flatter color index, whereas the outer parts of the galaxy tend to get redder with increasing radius.

**UGC 7165**: has a SBP that is close to an exponential, and also has a bright nuclear part. The color is almost constant over the whole radius range, apparently including the central part. But the resolution of our data is insufficient to discuss the center in any detail. The galaxy as a whole has a smooth elliptical appearance.

**UGC 7199**: knotty irregular with a central blue light excess. Exponential outer SBP shape, with a flat color profile outside the blue center.

**UGCA 276**: small galaxy with a faint central surface brightness. The central part is slightly deficient compared to an exponential. The color profile is flat.

**UGC 7298**: apparently small irregular galaxy with a knotty surface. Its color profile seems steep, being redder at large radius, but suffers from poor resolution and large error bars.

**UGC 7335**: elongated irregular galaxy with a bright central lane. The shape of the galaxy as a whole is elongated and elliptical. Its SBP is close to a pure exponential. The color profile is shallow, getting slightly redder with radius, and showing a bluing close to the center.

**UGC 7356**: classical nucleated dwarf elliptical. It has a published heliocentric radial velocity suggesting it is

close-by (but it is close in projection to NGC 4258). The brightest stars were not resolved by Makarova et al. (1998), confirming the dwarf elliptical nature. Its color profile is flat, with a slightly bluer nucleus.

**UGC 7369**: is a smooth, elliptically shaped galaxy, with a bright nucleus. It has a shallow color profile, becoming redder with radius, and a slightly blue nucleus. It is classified in the RC3 as an elliptical, but at $v_{\rm hel} = 333$ km s$^{-1}$ it could be a dwarf elliptical. Its SBP is close to exponential.

**UGC 7559**: irregular with a knotty face. Also seems disrupted, although not as severely as UGC 6817. We only have a $R$ frame. SBP close to an exponential, with a flat central part.

**UGC 7599**: apparently small irregular with a large central light excess above an exponential fit to the outer regions. Only a $B$ frame was available.

**UGC 7639**: irregular with a slight excess above an exponential in the inner part of its SBP. Knotty inner surface, and a slight luminosity excess to the north-west. Smooth color profile, showing a reddening with increasing radius.

Many authors report that color profiles show small gradients or are flat in dwarf galaxies (Bremnes et al. 1998; Patterson & Thuan 1996). We here find that all but two galaxies with color profiles show a reddening with increasing radius. UGC 6565 and UGC 7199 have a blue central part when compared to the outer parts. UGC 7047, UGC 7356 and UGC 7298 have flatter color gradients towards their centers. The remaining galaxies show monotonous color profiles.

To summarize, we have presented global photometric parameters for 15 galaxies in the Canes Venatici Cloud I in the $B$ and $R$ bands. Our sample corresponds to approx. one third of all galaxies in the direction of the cloud with heliocentric velocities less than 500 km s$^{-1}$.

*Acknowledgements.* T.B. and B.B. thank the Swiss National Science Foundation for financial support. We also thank Bernhard Parodi for taking part in the observing run.

This research has made use of the NASA/IPAC Extragalactic Database (NED) which is operated by the Jet Propulsion Laboratory, California Institute of Technology, under contract with the National Aeronautics and Space Administration, as well as NASA's Astrophysics Data System Abstract Service.

## References

Binggeli B., Cameron L.M., 1993, A&AS 98, 297
Binggeli B., Tarenghi M., Sandage A., 1990, A&A 228, 42
Bremnes T., Binggeli B., Prugniel P., 1998, A&AS 129, 313
Bremnes T., Binggeli B., Prugniel P., 1999, A&AS 137, 337
De Vaucouleurs G., 1959, Handbuch der Physik, Vol. 53, Flügge S. (ed.). Springer, Berlin, p. 275
Georgiev T.B., Karachentsev I.D., Tikhonov N.A., 1997, Astron. Lett. 23, 514
Karachentsev I.D., Drozdovsky I.O., 1998, A&AS 131, 1
Lesaffre P., Prugniel P., Binggeli B., Bremnes T., 1999 (in preparation)
Makarova L., Karachentsev I., Takalo L.O., Heinaemaeki P., Valtonen M., 1998, A&AS 128, 459
Makarova L.N., Karachentsev I.D., Georgiev T.B., 1997, Astron. Lett. 23, 378
Patterson R.J., Thuan T.X., 1996, ApJS 107, 103
Smith P.S., Balonek T.J., Heckert P.A., Elston R., Schmidt G.D., 1985, AJ 90, 1184
Tikhonov N.A., Karachentsev I.D., 1998, A&AS 128, 325